

**The Resolution Function  
of the  
High Resolution Backscattering Spectrometer  
at the Spallation Neutron Source**

K. W. Herwig  
Oak Ridge National Laboratory  
July 7, 2000

## I. INTRODUCTION

This instrument is a near-backscattering, crystal-analyzer spectrometer designed to provide extremely high energy resolution ( $\delta\omega \leq 2.6 \mu\text{eV}$  fwhm, elastic). The design requires a long initial guide section of 84 m from moderator to sample in order to achieve the timing resolution necessary to achieve the desired  $\delta\omega$ . The scattering chamber design is illustrated in Figure 1. Neutrons focused onto the sample by the supermirror funnel scatter towards the analyzer crystals. The strained perfect Si (111) crystals reflect neutrons with a very narrow distribution of energies centered at 2.082 meV onto the detectors. The design is optimized for quasielastic scattering but will provide 0.1% resolution in energy transfer,  $\omega$ , up to  $\omega = 18 \text{ meV}$ . This spectrometer will provide an unprecedented dynamic range near the elastic peak of  $-258 \mu\text{eV} < \omega < 258 \mu\text{eV}$ ,  $\sim$  seven times that of comparable reactor based instruments. For experiments that require the full dynamic range available at reactor based instruments (or greater), we expect this spectrometer to have an effective count rate  $\sim 100$  times that of the current best spectrometers.

The purpose of this document is to examine the resolution in energy transfer of the near backscattering spectrometer in more detail than previously described.[1] In particular, the term that depends on sample size and geometry will be discussed. The magnitude of this term can easily dominate the contributions from the incident flight path and analyzer crystals. Figure 1 gives a schematic view of the spectrometer.

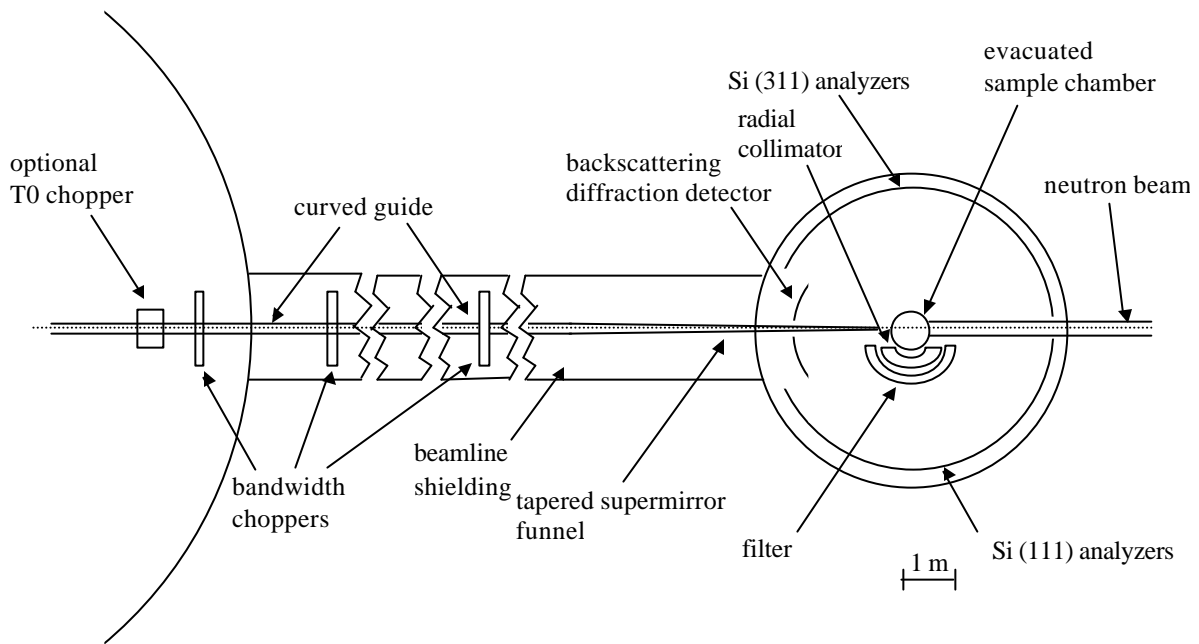


Figure 1. Schematic view of the backscattering spectrometer.

## II. RESOLUTION FUNCTION

The quantity of particular interest in this spectrometer is the resolution in energy transfer,  $\omega$ ,

$$\omega = E_i - E_f \quad 1$$

where  $E_i$  is the incident neutron energy and  $E_f$  is the final neutron energy. On a crystal analyzer spectrometer,  $E_f$  is fixed by Bragg reflection from the analyzer crystals and the incident energy is determined by neutron time of flight as

$$E_i = \frac{5.2276 \times 10^{-6} L_i^2}{(t - t_f - t_0)^2} \quad 2$$

where  $L_i$  is the moderator-sample distance,  $t$  is the total flight time as measured in a detector,  $t_f$  is the time for the neutron of known final energy to travel from the sample to analyzer to detector, and  $t_0$  is the emission time of the neutron from the moderator. The constant is correct for  $E_i$  in meV,  $L_i$  in m, and time in sec. The final neutron energy is given by

$$E_f = \frac{81.787}{4d^2 \sin^2(\theta_B)} \quad 3$$

where  $d$  is the d-spacing of the analyzer crystal and  $\theta_B$  is the analyzer Bragg angle. Differentiating Eqn. 1 gives the uncertainty in the energy transfer

$$\delta\omega = 2E_i \left( \frac{\delta L_i}{L_i} + \frac{\delta t_0 + \delta t_f}{t - t_f - t_0} \right) + 2E_f \left( \frac{\delta d}{d} + \cot(\theta_B) \delta\theta_B \right) \quad 4$$

The final neutron flight time is determined from

$$t_f = \frac{L_f 2d \sin(\theta_B)}{3955.4} \quad 5$$

where  $L_f$  is the flight path length from the sample-analyzer-detector. Differentiating Eqn. 5 gives the uncertainty in the final flight time

$$\delta t_f = t_f \left( \left( \frac{\delta L_f}{L_f} \right) + \left( \frac{\delta d}{d} \right) + (\cot(\theta_B) \delta\theta_B) \right) \quad 6$$

The terms in Eqn. 4 can be separated into those dependent on the primary spectrometer (components before the sample) and the secondary spectrometer (components after and including the sample). Taking the approximation that the terms are independent and that the uncertainties add in quadrature yields

$$\delta\omega = \sqrt{\delta\omega_P^2 + \delta\omega_S^2} \quad 7$$

where the contribution of the primary spectrometer to the resolution is

$$\delta\omega_P = 2E_i \left[ \left( \frac{\delta L_i}{L_i} \right)^2 + \left( \frac{\delta t_0}{t_i} \right)^2 \right]^{\frac{1}{2}} \quad 8$$

Typically, it is desirable to keep the first term in this equation small as compared to the second. The incident neutron flight time,  $t_i$ , is given in terms of the incident neutron wavelength,  $\lambda_i$ , as

$$\begin{aligned} t_i &= t - t_f - t_0 \\ &= \frac{L_i \lambda_i}{3955.4} \end{aligned} \quad 9$$

The contribution of the secondary spectrometer is

$$\delta\omega_S = 2 \left[ E_i^2 \left( \frac{\delta t_f}{t_i} \right)^2 + E_f^2 \left[ (\cot(\theta_B) \delta\theta_B)^2 + \left( \frac{\delta d}{d} \right)^2 \right] \right]^{\frac{1}{2}} \quad 10$$

Substituting Eqn. 6 for  $\delta t_f$  into Eqn. 10 (again taking the approximation that the terms are independent and add in quadrature) and separating the terms due to the analyzer crystals,  $\delta\omega_A$ , from those due to the finite sample size,  $\delta\omega_{FS}$ , yields

$$\delta\omega_S = \sqrt{\delta\omega_A^2 + \delta\omega_{FS}^2} \quad 11$$

$$\delta\omega_A = 2 \frac{\delta d}{d} \left[ \left( \frac{E_i t_f}{t_i} \right)^2 + E_f^2 \right]^{\frac{1}{2}} \quad 12$$

and

$$\delta\omega_{FS} = 2 \left[ \left( \frac{E_i t_f}{t_i} \frac{\delta L_f}{L_f} \right)^2 + \left( \left( \frac{E_i t_f}{t_i} \right)^2 + E_f^2 \right) \left( \cot(\theta_B) \delta\theta_B \right)^2 \right]^{\frac{1}{2}} \quad 13$$

### III. Various Contributions to the Resolution Function

In this section, each contribution to the resolution function is evaluated and compared for the case of elastic scattering,  $E_i = E_f$ . Table I lists the characteristic dimensions of the spectrometer.

Table I. Description of major components impacting the instrument resolution function.

Component	Description	Characteristic
Moderator	supercritical H <sub>2</sub> , poisoned,decoupled	$\delta t_0 = 45 \mu\text{sec}$ for $\lambda = 6.3 \text{ \AA}$
Incident Flight Path	10 cm (H) x 12 cm (V) supermirror Guide/Funnel	84 m from moderator to sample
Final Flight Path	Sample to Analyzer	nominally 2.52 m
	Analyzer to Detector	nominally 2.23 m
Analyzer Crystal	Bragg Angle	87.93 deg
	d-spacing	3.1354 \AA Si (111)
Sample	Geometry varied, design allows for cylinder filling beam cross section	3 x 3 cm <sup>2</sup> cross section of neutron beam

#### Moderator Emission Time Uncertainty, $\delta t_0/t_i$

This instrument will be located on a decoupled, poisoned, supercritical hydrogen, moderator, providing a polychromatic beam of cold neutrons to the instrument. For the current design, the moderator was taken as centerline poisoned which provides neutron pulse widths of

$$\delta t_0(\lambda) = \lambda \times 5.77 + 8.8 (\mu\text{sec}) \quad 14$$

for the wavelengths of use to this spectrometer. For  $\lambda = 6.267 \text{ \AA}$  (Si (111) analyzers) this corresponds to an emission time uncertainty of  $45 \text{ \mu sec}$ . The corresponding term in Eqn. 8 gives a contribution to the resolution of  $1.4 \text{ \mu eV}$ .

#### Incident Flight Path Uncertainty, $\delta L_i$

Figure 2 shows the result of a Monte Carlo simulation of the spectrometer guide system. In this simulation, a monochromatic beam ( $\lambda = 6.3 \text{ \AA}$ ) of neutrons was created at  $t = 0$  (no emission time uncertainty from the moderator) and allowed to propagate in the interior of a supermirror guide with a critical angle twice that of natural nickel. A converging funnel whose characteristics are given in Table 1 followed the supermirror guide. The neutrons were detected at the sample position. Figure 2 gives the time-of-flight dispersion arising from neutrons following different flight paths along the guide. This term is the incident flight path uncertainty and corresponds to a  $\delta L_i$  (fwhm) of  $0.57 \text{ cm}$ . The corresponding term in the resolution function in Eqn. 8 is only 0.20 that of the term due to the uncertainty in moderator emission time, and thus is insignificant in determining the resolution width.

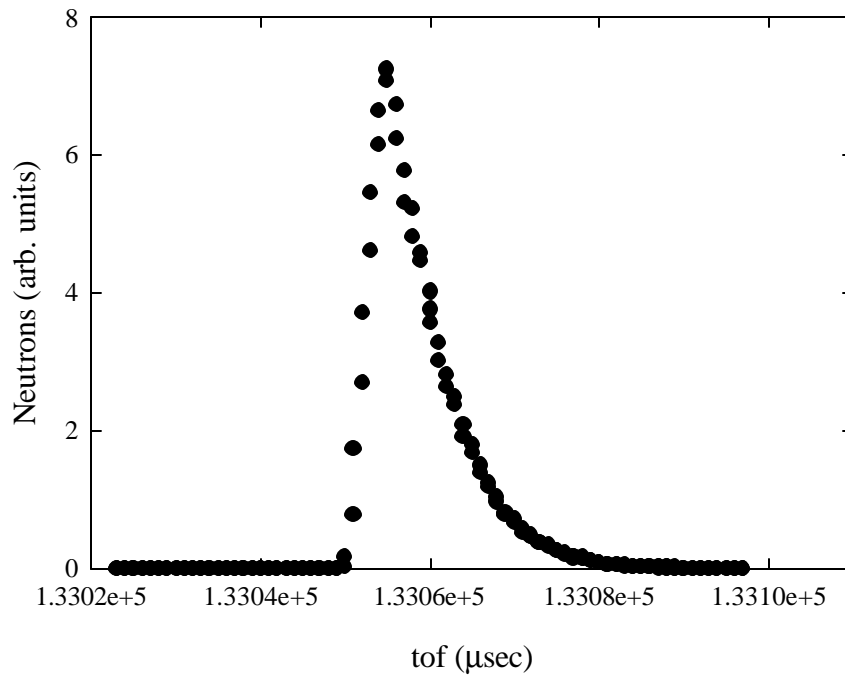


Figure 2. Timing uncertainty due to divergence in incident neutron beam. The time of flight is from the moderator surface to the sample position.

### Analyzer Crystal Contribution, $\delta d/d$

Because of the long incident flight path (84 m),  $t_i/t_f$  in Eqn. 12 is about 0.05. Thus, the first term in Eqn. 12 is negligible when compared to the second. Choosing  $\delta d/d = 3.5 \times 10^{-4}$ , gives a value of  $\delta\omega_A = 1.46 \mu\text{eV}$ , nearly matching the contribution from the incident flight path.

### Sample Dimension Contribution, $\delta\omega_{FS}$

The primary purpose of this document is to compare other terms in the resolution function to the contribution from sample size (Eqn. 13). Consider the first term in Eqn. 13, the uncertainty in final flight path distance that arises because of the finite sample size. This term varies with sample size and its magnitude can be estimated based on the geometry illustrated in Fig. 3. One can integrate over the sample dimensions and generate the distribution of sample-analyzer flight path distances as shown in Fig.4 for a sample dimension of  $3 \times 3 \text{ cm}^2$  and a nominal flight path of 2.5 m. Figure 5 shows the distribution of Bragg angles for a nominal Bragg angle of  $88 \text{ deg}$  as seen from the center of the sample.

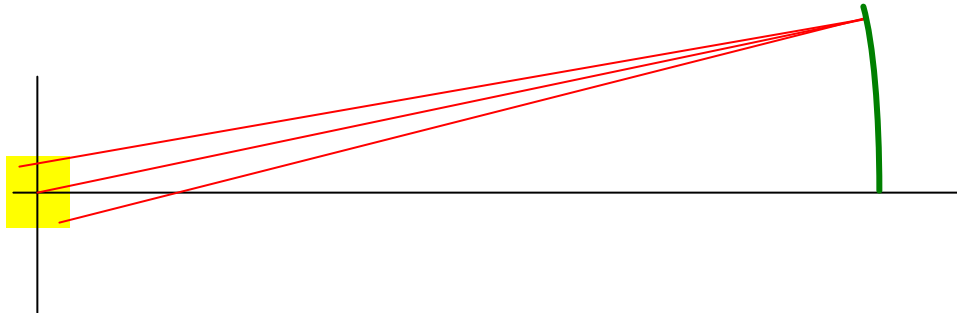


Figure 3. Flight path uncertainty due to finite sample size.

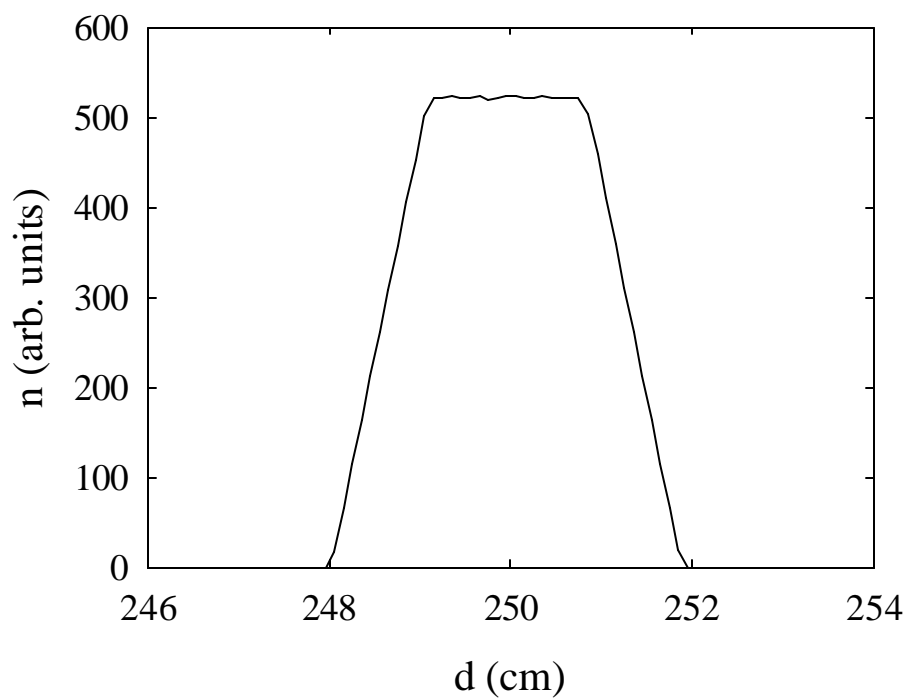


Figure 4. Distribution of sample-analyzer distances for a  $3 \times 3 \text{ cm}^2$

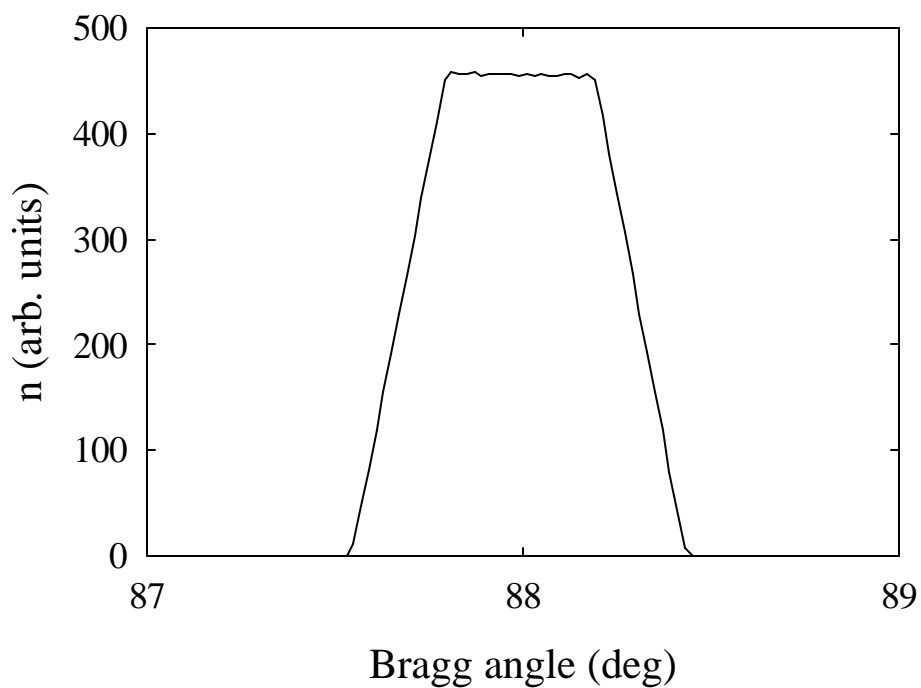


Figure 5. Distribution of Bragg angles for a  $3 \times 3 \text{ cm}^2$  sample, a nominal Bragg angle of 88 deg, and a nominal sample-analyzer distance

Figure 6 illustrates the geometry involved in calculating the relevant terms in Eqn. 13. The point  $(x_c, y_c)$  is the center of rotation in the vertical dimension for the analyzer crystals. The Bragg angle varies slightly with position on the sample and position on the analyzer but is given by  $90 - \beta$ . Two final flight paths are outlined in green, while the radius of curvature of the analyzer crystals is drawn in red. In general, the detector may be inclined with respect to the normal to the scattering plane and this angle is  $\alpha$ .

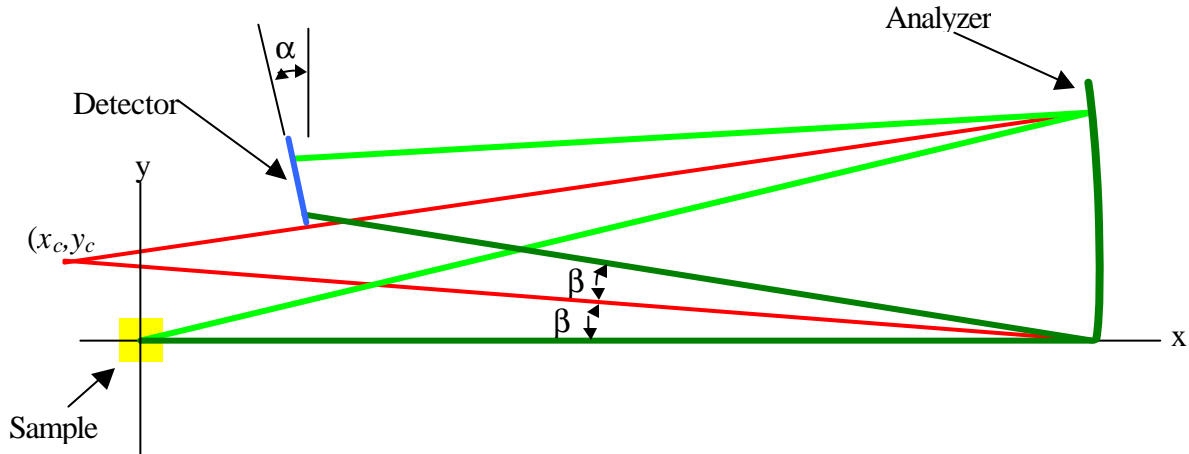


Figure 6. Sample/Analyzer Crystal geometry.

The detector tilt angle can be chosen so as to minimize variations in the total final flight path distance,  $L_f$ . As seen in Fig. 4 this variation can be dominated by sample size, however, for small samples, the tilt angle plays an important role. This can be seen in Fig. 7 showing the behavior of  $\delta\omega_{FS}$  as a function of tilt angle for a  $1 \times 1 \text{ cm}^2$  sample. As intended for this spectrometer, another approach that reduces this effect is to choose a position sensitive detector. However, even for this choice of detector, choosing the correct  $\alpha$  may prove to be beneficial in cases where the analyzer crystals may be slightly misaligned. As seen in Figure 7, the desirable angle is  $\alpha = 7 \text{ deg}$ .

Figure 8 shows the behavior of  $\delta\omega_{FS}$  as a function of  $(x_c, y_c)$  the center of rotation of the analyzer crystals. The uncertainties in both  $L_f$  and  $\delta\theta_B$  and the Bragg angle itself vary with this parameter. As expected, the minimum in this term arises when the center of rotation approaches the origin of the sample. In this case, the geometry is nearly exact backscattering, and the detectors would need to be placed on the opposite side of the sample. In fact, the minimization of the terms in Eqn. 13 is restricted by engineering constraints. The spectrometer design calls for a vertical acceptance of the analyzer system of  $\pm 22 \text{ deg}$  from the scattering plane. As one travels on the surface in Fig. 8 towards the origin, the Bragg angle approaches  $90 \text{ deg}$ , and the bottom of the detector must be located at lower values of  $y$  (see Fig. 6), blocking neutrons that would otherwise reach the top of the detector. For practical considerations, there must be some distance

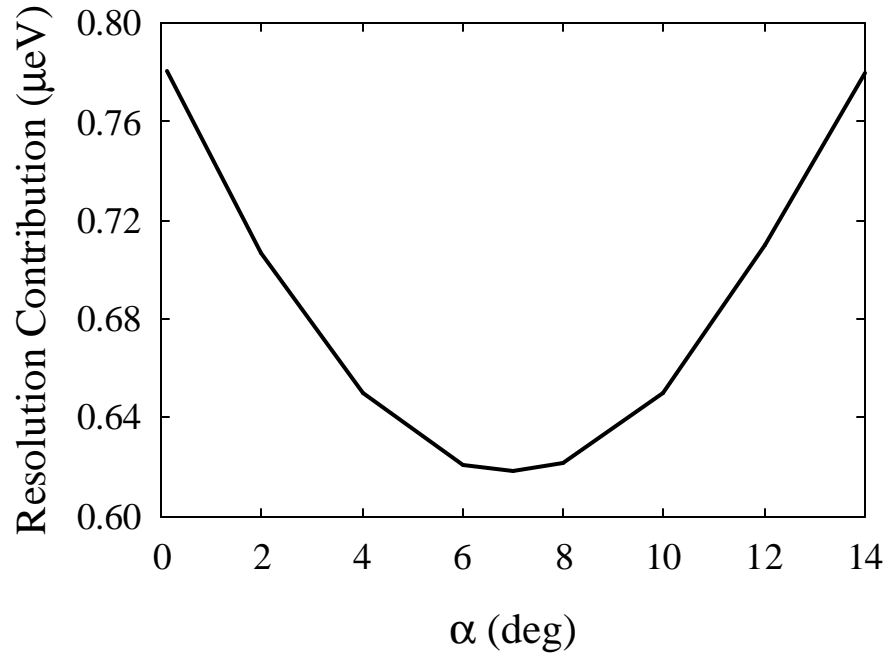


Figure 7. Resolution contribution of Eqn. 13 for a  $1 \times 1 \text{ cm}^2$  sample as a function of detector tilt angle.

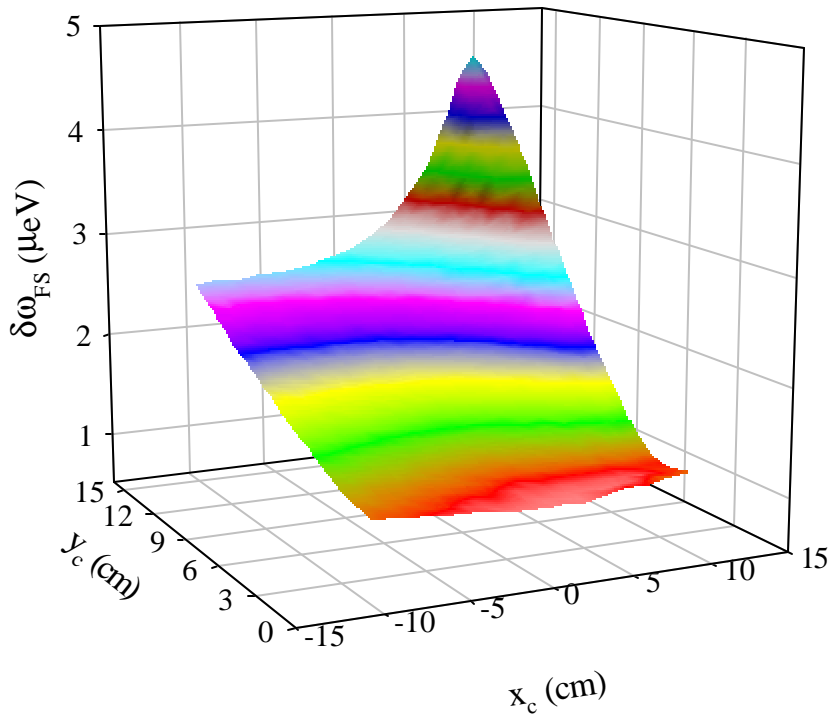


Figure 8. Resolution contribution,  $\delta\omega_{\text{FS}}$ , for a 250 cm nominal sample-analyzer distance as a function of the vertical center-of-rotation of

preserved from the active end of the detector to the path of neutrons traveling from the sample to the top of the analyzer system. Figure 9 shows this distance,  $d_{DN}$ , as a function of  $(x_c, y_c)$ . Negative values of this term would require the detectors to be placed on the opposite side of the sample, limiting the spectrometer use to a single side. The minimum practical value for this term has been set at  $\sim 4$  cm. A value of  $(x_c, y_c) = (-1.6, 9)$  gives the lowest  $\delta\omega_{FS}$ ,  $1.77 \mu\text{eV}$ , that achieves a  $d_{DN}$  of 4 cm.

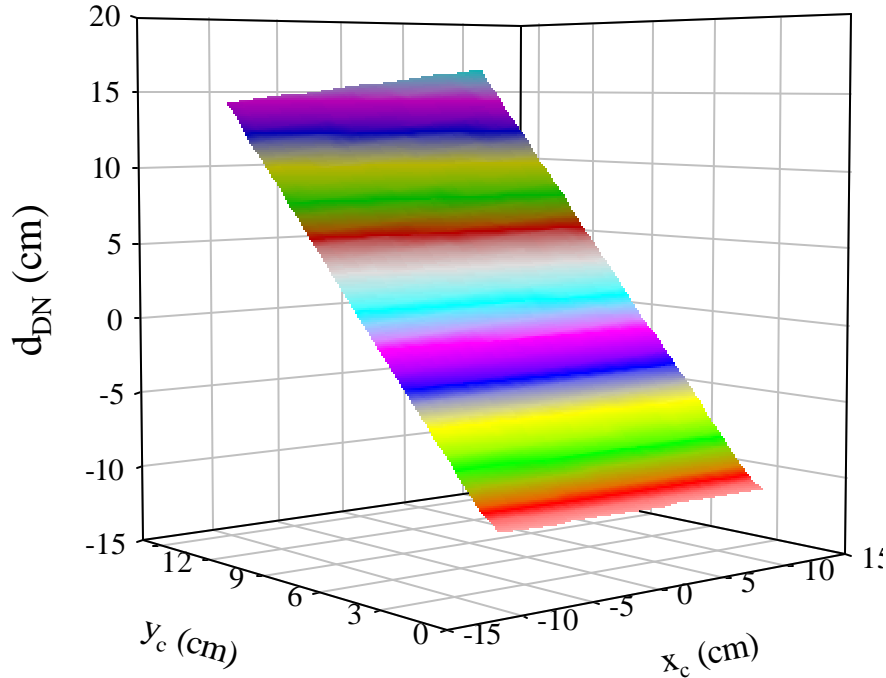


Figure 9. The distance from the lower edge of the detector to the neutron beam from the sample to the upper edge of the

Figure 10 shows  $\delta\omega_{FS}$  and the total instrument resolution as a function of sample size. The nominal sample size that the guide system has been designed for is  $3 \times 3 \text{ cm}^2$ . The resolution can be improved, however, by choice of a smaller sample at the expense of neutron counts in the detectors. I note that Figure 10 shows the worst case geometry for a rectangular slab sample as the sample is viewed edge on. In reality, such a sample would likely be oriented at  $45^\circ$  with respect to the incident neutron beam. At a  $45^\circ$  scattering angle,  $\delta\omega_{FS}$  is  $0.6 \mu\text{eV}$  (total resolution =  $2.1 \mu\text{eV}$ ) compared to  $1.77 \mu\text{eV}$  (total resolution =  $2.7 \mu\text{eV}$ ) for the sample viewed edge on. The values shown in Figure 10 should also represent bounds on the expected resolution for cylindrical samples as well.

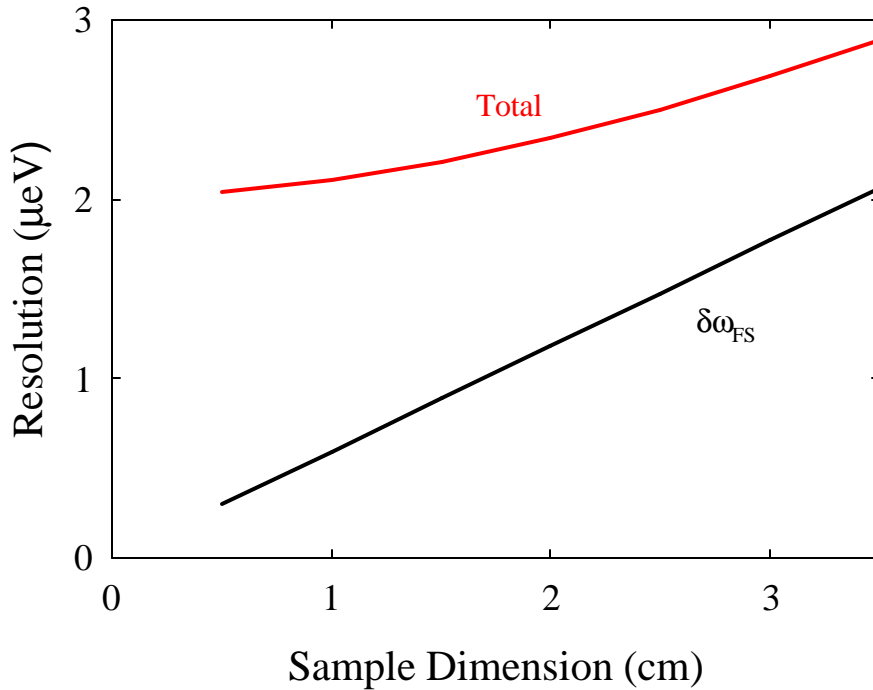


Figure 10. Resolution as a function of sample

#### IV. CONCLUSION

In conclusion, the resolution function of this instrument will depend on sample size and geometry. At the sacrifice of counting rate, smaller samples can be used to improve the resolution of the spectrometer over a practical range of 2.2  $\mu\text{eV}$  to 2.7  $\mu\text{eV}$ . Changing the spectrometer design to incorporate a larger flight path would lessen the effect of sample dimension on the resolution. However, a larger flight path significantly impacts the total cost of the spectrometer. For example, increasing the nominal sample-analyzer distance to 3.0 m from 2.5 m increases the analyzer surface area from 18  $\text{m}^2$  to 27  $\text{m}^2$  at a cost of \$900k. The size of the scattering tank would also increase adding additional cost.

The detectors should be tilted 7 deg out of the scattering plane in order to optimize the resolution for small samples ( $\sim 1 \times 1 \text{ cm}^2$ ), although this effect is negligible compared to other terms for large samples ( $\sim 3 \times 3 \text{ cm}^2$ ). This is a small effect, but the cost of tilting the detectors is insignificant.

**REFERENCES**

- [1] K. W. Herwig, "Conceptual Analysis for the Backscattering Spectrometer at the Spallation Neutron Source", SNS Document number ES-1.1.8.4-6017-RE-A-00, 1999.